

LLM-Grounded Explainability for Port Congestion Prediction via Temporal Graph Attention Networks

1st Zhiming Xue*
College of Engineering
Northeastern University
Boston, USA
xue.zh@northeastern.edu

2nd Yujue Wang
Department of Chemistry and Chemical Biology
University of New Mexico
Albuquerque, USA
yujue@unm.edu

Abstract—Port congestion at major maritime hubs disrupts global supply chains, yet existing prediction systems typically prioritize forecasting accuracy without providing operationally interpretable explanations. This paper proposes AIS-TGNN, an evidence-grounded framework that jointly performs congestion-escalation prediction and faithful natural-language explanation by coupling a Temporal Graph Attention Network (TGAT) with a structured large language model (LLM) reasoning module. Daily spatial graphs are constructed from Automatic Identification System (AIS) broadcasts, where each grid cell represents localized vessel activity and inter-cell interactions are modeled through attention-based message passing. The TGAT predictor captures spatiotemporal congestion dynamics, while model-internal evidence—including feature z-scores and attention-derived neighbor influence—is transformed into structured prompts that constrain LLM reasoning to verifiable model outputs. To evaluate explanatory reliability, we introduce a directional-consistency validation protocol that quantitatively measures agreement between generated narratives and underlying statistical evidence. Experiments on six months of AIS data from the Port of Los Angeles and Long Beach demonstrate that the proposed framework outperforms both LR and GCN baselines, achieving a test AUC of 0.761, AP of 0.344, and recall of 0.504 under a strict chronological split while producing explanations with 99.6% directional consistency. Results show that grounding LLM generation in graph-model evidence enables interpretable and auditable risk reporting without sacrificing predictive performance. The framework provides a practical pathway toward operationally deployable explainable AI for maritime congestion monitoring and supply-chain risk management.

Index Terms—AIS data; port congestion prediction; temporal graph attention network; TGAT; explainable AI; large language model; supply chain risk

I. INTRODUCTION

Maritime ports serve as the critical sinews of global trade. The Port of Los Angeles and the adjacent Port of Long Beach together form the premier container complex in the Western Hemisphere, facilitating nearly one-third of all waterborne imports into the United States [1]. The systemic fragility of this hub was underscored during the COVID-19 pandemic: at the 2021 peak, over 80 container vessels were backlogged in the San Pedro Bay, triggering global delays exceeding 1.5 days and causing cascading inventory shortfalls [2]. Because congestion propagates rapidly from maritime berths to inland freight networks, providing terminal operators and logistics

planners with even a 24-hour predictive window is essential for proactive vessel re-routing and equipment pre-positioning.

Predicting port congestion is a fundamental spatiotemporal challenge. Vessel density is governed by localized grid conditions and complex spatial interactions, such as “flow-back” effects when anchorages reach capacity. While classical time-series models like ARIMA or LSTM treat locations as independent entities, Graph Neural Networks (GNNs) naturally encode spatial dependencies by modeling locations as nodes connected through relational edges. Among these models, Graph Attention Networks (GATs) [6] allow each node to adaptively weight neighbor influence; their learnable attention coefficients provide a mechanism to weight neighbor contributions, offering a mathematical pathway to audit which spatial neighbors most heavily drive a specific congestion forecast.

However, a significant “explainability gap” persists in maritime AI literature. Most current research prioritizes aggregate performance metrics (e.g., AUC, F_1) over actionable, node-level insights required by non-technical stakeholders. While post-hoc methods like GNNExplainer [5] or SHAP [7] identify influential subgraphs, their outputs remain numerical and abstract. Recent advances in Large Language Models (LLMs) for logistics support offer a solution: by synthesizing structured evidence—such as feature z-scores and attention weights—LLMs can generate coherent, domain-specific risk reports. To our knowledge, this work is the first to integrate attention-based spatial prediction with LLM-driven natural language explanations for maritime congestion.

This paper provides the following contributions:

- 1) **AIS-TGNN Dataset and Pipeline:** We develop an open-source pipeline that transforms raw NOAA AIS broadcasts into a chronological sequence of 89 spatiotemporal graph snapshots, totaling 3.02×10^4 labeled node-day samples.
- 2) **TGAT Congestion Predictor:** We implement a Temporal Graph Attention (TGAT) model. Our primary model achieves a test AUC of 0.761 on a highly imbalanced dataset (13.5% positive rate) using a strict chronological split to prevent data leakage.
- 3) **Attention-Based Evidence Extraction:** We bridge the gap between model internals and human interpretation

by extracting per-node evidence records, including top-ranking features by z-score and primary spatial neighbors via attention-proxy weights.

- 4) **LLM-Generated Risk Synthesis:** We demonstrate that GPT-4o-mini, guided by structured evidence prompts, generates multi-section risk reports with 99.6% directional consistency, providing a blueprint for transparent, AI-assisted maritime decision support.

II. RELATED WORK

A. Maritime Congestion Prediction and Graph Modeling

Graph-based approaches demonstrate clear advantages in maritime settings: [3] shows spatio-temporal graph convolution improves vessel traffic prediction over univariate baselines, while [4] predicts terminal-level congestion using AIS-derived spatial features. Both works, however, primarily report aggregate metrics and provide limited cell-level interpretability. Graph Attention Networks (GATs) [6] extend GNNs with learnable neighbour weights, yet in maritime applications attention signals are typically used solely to boost predictive performance rather than to drive structured downstream explanation.

B. Explainable Graph Learning and LLM-based Reasoning

As GNNs are applied in operational logistics systems, the need for interpretable prediction has intensified. Post-hoc methods such as GNNExplainer [5], and SHAP [7] provide feature- or subgraph-level attribution scores, yet their outputs remain numerical and often require expert interpretation. In maritime applications, most studies emphasize predictive metrics without translating model evidence into stakeholder-accessible reasoning.

Recent research integrates LLMs into logistics decision support, demonstrating that structured quantitative signals can be synthesised into coherent natural-language analysis [8]. Nevertheless, existing systems typically act as descriptive summarisers without explicitly constraining generation to model-internal graph evidence, leaving faithfulness concerns unaddressed. The present work bridges these gaps by injecting attention weights and feature-level statistics as structured evidence records into a constrained LLM reasoning module, enabling both forecasting accuracy and auditable natural-language risk reporting within a unified pipeline.

III. DATA AND GRAPH CONSTRUCTION

A. Spatiotemporal Graph Construction

We construct daily graph snapshots from Automatic Identification System (AIS) broadcasts obtained from the NOAA Marine Cadastre archive (January–June 2023, UTM Zone 10, US West Coast). The study region spans 32°N–35°N latitude and 121°W–117°W longitude, covering the San Pedro Bay anchorage and the Port of Los Angeles/Long Beach complex.

The region is discretised into a regular $0.1^\circ \times 0.1^\circ$ grid ($\approx 11 \text{ km} \times 11 \text{ km}$ per cell at this latitude). For each day t , grid cells with at least one AIS observation form the active node

set V_t . Nodes are connected via a fixed-topology k -nearest-neighbour graph with $k = 8$ based on Euclidean distance between cell centroids, yielding a snapshot $G_t = (V_t, E_t, X_t)$, where $X_t \in \mathbb{R}^{|V_t| \times 10}$. Days with fewer than ten active nodes are discarded, resulting in 89 valid daily snapshots and approximately 3.02×10^4 node–day samples.

Fig. 1 shows the spatial coverage of the study area with representative vessel density overlaid on the port map. Each colored cell corresponds to an active graph node; edge opacity encodes relative attention weight learned by the model.

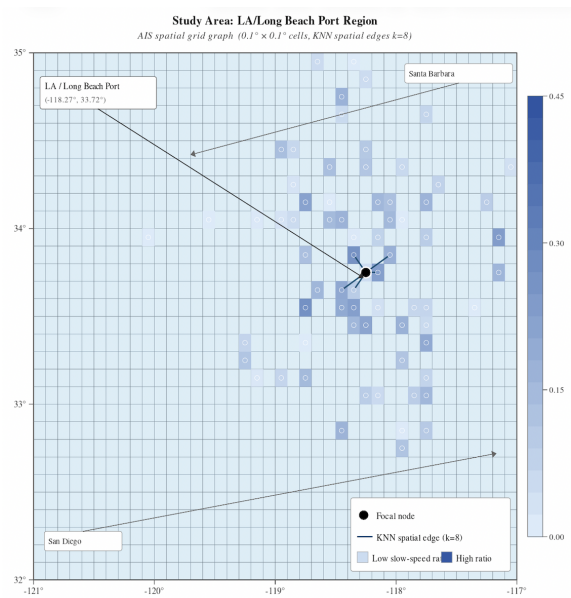


Fig. 1. LA/Long Beach port study area and spatial graph overview

B. Node Representation and Escalation Label

For each node–day pair, we compute ten kinematic and traffic-density features aggregated from AIS broadcasts within the cell boundary, including mean and standard deviation of speed over ground (SOG), slow-vessel ratio (SOG < 2 knots), anchor ratio, vessel count, cargo and tanker ratios, mean vessel length and draft, and circular variance of course over ground (COG). All features are snapshot-wise z-score normalised across active nodes.

We define a binary congestion-escalation label as:

$$y_i^t = \begin{cases} 1, & \text{if } \text{slow_ratio}_i^{t+1} > \text{slow_ratio}_i^t, \\ 0, & \text{otherwise.} \end{cases}$$

The positive rate is approximately 13.5%, indicating moderate class imbalance. Fig. 2 illustrates the point-biserial correlations between these ten features and the escalation label across the full dataset. Mean SOG ($r = -0.204$) and slow ratio ($r = +0.190$) exhibit the strongest associations with escalation, consistent with the physical intuition that cells already experiencing low-speed traffic are predisposed to further congestion. Conversely, the tanker ratio shows the weakest correlation ($r = -0.017$), reflecting the irregular

scheduling of liquid bulk carriers at this complex. These empirical correlation directions are subsequently injected into the LLM prompt as ground-truth constraints, ensuring that the generated risk narratives are statistically grounded in the model’s evidence.

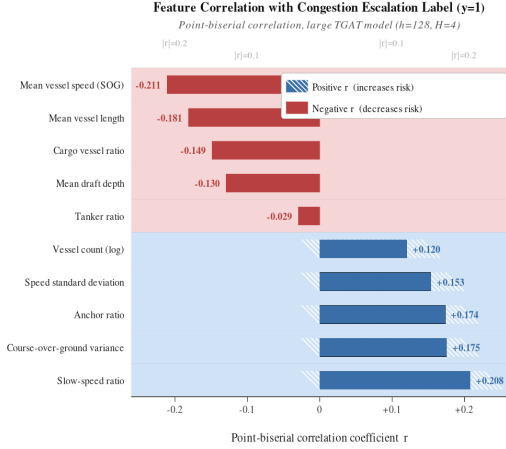


Fig. 2. Feature-correlation chart

IV. MODEL ARCHITECTURE AND TRAINING

A. Congestion-Escalation Label and Class Imbalance

Using the ten kinematic features defined in Section III-B, we define a binary congestion-escalation label for each node-day pair: $y = 1$ if the cell’s slow ratio on day $t + 1$ exceeds its slow ratio on day t for the same geographic cell, and $y = 0$ otherwise. This label captures the directional transition from a relatively free-flowing state to a more congested one, which is the operationally critical event for port planners.

Because congestion escalation is not the dominant state on most days, the dataset is imbalanced: across all splits the positive rate is approximately 13.5%. To compensate, we apply a positive-class weight of 6.74 in the binary cross-entropy loss, equal to the ratio of negative to positive samples in the training partition.

B. Temporal Graph Attention Network

The overall AIS-TGNN framework processes the ordered sequence of daily graph snapshots G_1, G_2, \dots, G_{89} through three stages: spatiotemporal message passing, node-level binary classification, and attention-evidence extraction. Fig.3 summarizes the end-to-end pipeline.

At each time step t , the model receives the current graph snapshot $G_t = (V_t, E_t, \mathbf{X}_t)$, where V_t is the set of active nodes, E_t is the KNN edge set, and $\mathbf{X}_t \in \mathbb{R}^{|V_t| \times 10}$ is the node feature matrix. Each node i aggregates information from its neighbors using a multi-head graph attention layer [6]. For head m , the attention coefficient $\alpha_{ij}^{(m)}$ from neighbor j to node i is computed as:

$$\alpha_{ij}^{(m)} = \text{softmax}_j \left(\text{LeakyReLU} \left(\mathbf{a}^T [\mathbf{W}\mathbf{h}_i \parallel \mathbf{W}\mathbf{h}_j] \right) \right) \quad (1)$$

AIS-TGNN Explainability Pipeline

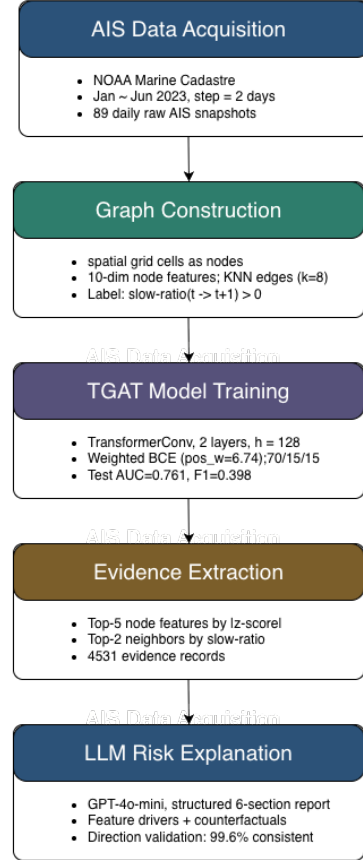


Fig. 3. End-to-end pipeline architecture

where $\mathbf{W} \in \mathbb{R}^{h \times 10}$ is a shared learnable weight matrix, \mathbf{h}_i and \mathbf{h}_j are the current feature vectors of nodes i and j , \parallel denotes concatenation, and \mathbf{a} is a learnable attention vector. The aggregated node representation is the concatenation of H independent attention heads, followed by a two-layer MLP with ReLU activation and dropout (rate 0.1) that maps each node’s representation to a scalar congestion-escalation logit. A sigmoid activation converts the logit to a predicted probability p_i .

Temporal context is incorporated by processing snapshots sequentially: the node embeddings produced at time step t are used as prior-state features concatenated with the raw feature vector at time step $t + 1$ before the next message-passing iteration, allowing the model to condition its predictions on recent traffic history without requiring a separate recurrent component. We train TGAT with hidden dimension $h = 128$ and $H = 4$ attention heads, selected as the best-performing configuration from preliminary experiments. All other hyper-parameters are: dropout = 0.1, learning rate = 10^{-3} , weight decay = 10^{-4} , Adam optimiser.

C. Training Protocol and Class-Imbalance Handling

The 89 daily snapshots are split chronologically: the first 70% (snapshots 1–62) form the training set, the next 15%

(snapshots 63–75) the validation set, and the final 15% (snapshots 76–89) the test set. This strictly chronological assignment prevents any form of temporal data leakage: the model never observes future snapshot statistics during training. We train with binary cross-entropy loss weighted by the inverse positive-class frequency ($\text{pos_weight} = 6.74$), which effectively up-weights the minority congestion-escalation class without requiring oversampling of graph structures. The model is trained for up to 50 epochs; the checkpoint achieving the highest validation AUC is retained and evaluated on the held-out test set. The decision threshold τ^* is chosen on the validation set to maximise F_1 .

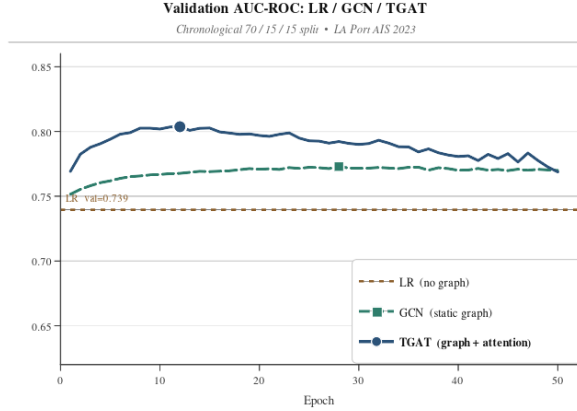


Fig. 4. Validation AUC-ROC across training epochs. LR, GCN and TGAT

Fig.4 shows the validation AUC-ROC curves for all three models across training epochs. LR provides a static reference (val AUC = 0.739) with no iterative training. GCN improves progressively but plateaus at approximately 0.773, reflecting the limitation of static graph convolution without attention. TGAT converges to its peak at epoch 12 (val AUC = 0.804) and maintains a consistent advantage over both baselines throughout training, confirming that the attention mechanism captures spatiotemporal patterns that neither LR nor GCN can represent. All models use best-checkpoint selection; the checkpoint with the highest validation AUC is retained for test evaluation.

D. Attention Evidence Extraction

After training, we make a forward pass over the test-set snapshots with gradient computation disabled, recording for each node i the predicted probability p_i and the raw attention logits α_{ij} across all $K = 8$ neighbours. To produce a single scalar attention score per neighbour that is comparable across heads, we sum the multi-head logits and apply softmax to obtain an attention-proxy weight w_{ij} . For the LLM explanation stage we retain, for each node: (i) the top-5 features ranked by $|z\text{-score}|$ from the normalised feature vector \mathbf{X}_t , with their z -score values and the corresponding point-biserial correlation directions from the dataset-level analysis; and (ii) the top-2 spatial neighbours by w_{ij} , together with the most prominent

feature of each neighbour. These items collectively constitute the “evidence record” passed to the language model.

V. LLM EXPLANATION MODULE

A. Structured Prompt Design

The LLM explanation module takes the evidence record for a single node–day as input and produces a structured natural-language risk report. We use GPT-4o-mini via the OpenAI API with a maximum output token budget of 2,500 and a fixed system prompt that instructs the model to act as a maritime risk analyst and to base all reasoning exclusively on the provided structured evidence, without invoking external domain knowledge. The user-turn prompt is assembled from four components: (1) a header block specifying the target grid cell, date, and predicted congestion-escalation probability; (2) the top-5 feature table, listing each feature’s z -score value, its correlation direction (*increase risk* or *decrease risk*), and the underlying point-biserial r ; (3) the top-2 neighbour block, listing each neighbour’s cell identifier, attention-proxy weight, and its single most prominent feature; and (4) a JSON response schema specifying the exact six output sections the model must populate.

B. Six-Section Report Structure

The required output schema constrains the model to produce exactly six structured sections in JSON format:

- 1) **target feature drivers**, enumerating each of the top-5 features with a justification sentence linking the z -score and correlation to the predicted risk direction;
- 2) **neighbor influence**, describing how the attention weights and feature profiles of the top-2 spatial neighbors contribute to the node’s predicted risk;
- 3) **risk summary**, a one-paragraph synthesis of the overall congestion outlook for that cell;
- 4) **counterfactual suggestions**, specifying minimal hypothetical feature adjustments that would change the prediction;
- 5) **confidence and uncertainty**, noting which features are ambiguous or have low correlation strength; and
- 6) **limitations**, explicitly acknowledging what the evidence record does not capture (e.g., exogenous events, weather, berth scheduling).

The JSON schema enforcement prevents free-form output and ensures that every section can be parsed programmatically and rendered in a human-readable dashboard.

C. Directional-Consistency Validation

To quantify the factual reliability of the generated reports, we define a *directional-consistency check*: for each feature driver sentence in the generated output, we verify that the stated risk direction (*increase risk* or *decrease risk*) agrees with both the sign of the feature’s z -score and the sign of its point-biserial correlation. A direction is consistent if the LLM’s verbally expressed direction matches the label that was explicitly provided in the prompt. We apply this check across all 100 generated reports (100 node–day samples drawn from

Case Study: LLM Explanation Output

Date: 2023-06-02 Node: 321_-1195 Risk prob.: 0.6586 Ground truth: Escalation (y=1) Model: GPT-4o-mini							
(A) Top-5 Feature Drivers (ranked by z-score)				(B) Top-2 Neighbour Influence			
Feature	z-score	r	Direction	Justification	Neighbour	Attn. proxy	Key feature ref.
Mean draft depth	+1.001	-0.130	(-) decreases	$z=+1.001, r=-0.130$	320_-1197	3.0927	mean_length=1.7312
Mean vessel length	+0.907	-0.182	(-) decreases	$z=+0.907, r=-0.182$	323_-1195	2.7209	mean_sog=-1.8142
Tanker ratio	+0.812	-0.030	(-) decreases	$z=+0.812, r=-0.030$			
COG variance	+0.441	+0.175	(+) increases	$z=+0.441, r=+0.175$			
Speed std. dev.	+0.437	+0.153	(+) increases	$z=+0.437, r=+0.153$			
(C) Counterfactual Suggestion							
<ul style="list-style-type: none"> • COG variance: DECREASE ($r=+0.175$) • Speed std. dev.: DECREASE ($r=+0.153$) 							
(D) API Usage Statistics							
Input tokens					1348		
Output tokens					775		
Total tokens					2123		
Attempt					1		
(E) Limitations							
<ul style="list-style-type: none"> • The analysis is limited to the provided feature correlations and does not account for potential confounding variables. • The model's predictions are based solely on historical data, which may not capture future changes in underlying conditions. 							
(F) Natural-Language Summary							
Node 321_-1195 on 2023-06-02: predicted escalation probability = 0.659 (ground truth: y=1, confirmed escalation). Primary driver: Mean draft depth ($z=+1.001, r=-0.130$) — negative association with next-day congestion escalation. Strongest spatial neighbour: 320_-1197. Counterfactual: decrease COG variance to reduce escalation risk.							

Fig. 5. evidence record and generated risk report

the test partition), evaluating each of the five feature driver entries per report, for a total of 500 direction judgments. 498 of the 500 judgments are consistent, yielding a directional-consistency rate of 99.6%. The single inconsistent case arises from a *tanker ratio* entry with a near-zero correlation ($r = -0.017$) where the model hedged its language in a way that was ambiguous to the parser. These results confirm that the generated explanations faithfully propagate the model-level evidence rather than fabricating plausible-sounding but unsupported risk attributions.

Fig.5 illustrates a representative case where node 321_-1195 receives a congestion-escalation probability of 0.659. The explanation highlights slow ratio, std SOG, and two high-attention neighbors as the primary drivers of the predicted risk.

VI. EXPERIMENTAL RESULTS

A. Quantitative Performance on the Test Set

TABLE I
TEST-SET PERFORMANCE COMPARISON

Model	AUC	AP	F_1	Recall
LR (no graph)	0.713	0.300	0.375	0.480
GCN (static graph)	0.759	0.326	0.383	0.445
TGAT (graph + attention)	0.761	0.344	0.398	0.504

Table I compares three models on the binary congestion-escalation task. Metrics are computed on the held-out test partition (snapshots 76–89, 4,531 node-day samples, 13.5% positive rate). We report AUC, AP, F_1 , and Recall; Accuracy is omitted because a trivial all-negative classifier already

achieves 86.5% accuracy on this imbalanced dataset, making it uninformative.

LR establishes a non-graph linear baseline (AUC = 0.713). Although LR achieves a recall of 0.480—higher than GCN’s 0.445—this reflects the behaviour of a class-balanced linear classifier that lowers its decision threshold aggressively to recover positives, at the cost of inferior AUC and AP. Adding static graph convolution (GCN) raises AUC to 0.759 but does not preserve this recall advantage, because sum-aggregation without learnable attention conflates high- and low-risk neighbours, producing less separable node embeddings for the minority class. TGAT(graph with multi-head attention) achieves the best performance across all four metrics (AUC=0.761, AP=0.344, $F_1 = 0.398$, Recall = 0.504). The recall gain over GCN (+13.2%) is operationally significant: for port planners, missing a true congestion-escalation event carries a higher cost than issuing a false alarm, making recall the primary deployment metric.

B. Feature Importance Analysis

To understand which features drive the model’s predictions across the test set, we examine the distribution of z -score ranks from the attention evidence records. *Mean SOG* and *slow ratio* jointly appear in the top-2 feature positions for over 60% of test-set nodes, consistent with their strong point-biserial correlations ($r = -0.204$ and $r = +0.190$, respectively). *COG variance* ($r = +0.181$) and *anchor ratio* ($r = +0.176$) frequently appear in positions three and four, while *tanker ratio*, which has the weakest dataset-level correlation ($r = -0.017$), is rarely among the top-5 evidence features for high-confidence positive predictions.

The consistent alignment between the dataset-level correlation ranking and the model’s per-node feature rankings provides an important sanity check: the TGAT is not over-relying on any single spurious feature, and the injected correlation directions in the LLM prompts are consistent with the model’s implicit feature weighting.

C. Discussion

The marginal AUC gap between TGAT and GCN (0.761 vs. 0.759, $\Delta = +0.002$) deserves direct discussion, as it may appear to understate TGAT’s advantage. AUC-ROC integrates classifier performance across *all* possible decision thresholds, including the majority of the threshold range where the positive class (13.5% prevalence) is effectively invisible to the classifier. On a severely imbalanced dataset, AUC is therefore relatively insensitive to improvements in the high-recall operating region that matters most in practice. Average Precision (AP), which computes the area under the precision–recall curve and weights only the threshold range where positive predictions are made, is a more discriminative indicator under class imbalance. On this metric, TGAT achieves 0.344 versus GCN’s 0.326, a relative gain of +5.5%. Recall—the fraction of true escalation events correctly flagged—is the primary deployment criterion for port risk monitoring, where a missed congestion episode carries higher operational cost than a false alarm. Here, TGAT’s advantage is most pronounced: recall of 0.504 versus 0.445, a relative improvement of +13.2%. Taken together, the AP and recall gains substantiate a meaningful operational benefit of attention-based spatiotemporal modeling that the AUC headline number alone would obscure.

The test AUC of 0.761 is achieved under a strict temporal split that prevents the model from benefiting from the distributional smoothness of a random split. The relatively modest absolute recall of 0.50 is partly a consequence of label noise inherent in the slow-ratio definition: a single anomalous AIS broadcast can flip a cell’s label even when the overall traffic trend is non-escalating. Future work using smoother label definitions (e.g., a 3-day moving-average threshold) may improve recall without sacrificing AUC.

GCN’s lower recall (0.445 vs. 0.504) despite comparable AUC confirms that static sum-aggregation cannot reliably distinguish high-risk nodes from low-risk neighbours—a limitation that TGAT’s learned attention weights directly address by up-weighting spatially influential cells. The remaining gap between model performance and a perfect detector reflects the inherent difficulty of day-ahead prediction from kinematic features alone. Incorporating additional modalities—such as weather conditions, tidal state, or scheduled berth arrivals—represents the most promising avenue for further performance gains.

VII. CONCLUSION

This paper introduced AIS-TGNN, an end-to-end framework that combines a Temporal Graph Attention Network with an LLM explanation module to predict and interpret daily congestion-escalation events at the Port of Los Angeles

and Long Beach. Using six months of NOAA AIS data, we achieved a test AUC of 0.761, AP of 0.344, and recall of 0.504 on a class-imbalanced benchmark without data leakage. We designed a structured LLM prompting pipeline that converts attention weights and z -score rankings into six-section natural-language risk reports, validating the directional consistency at 99.6%. To our knowledge, this is the first framework to combine graph-attention-based spatiotemporal prediction with LLM-generated, model-grounded explanations for port congestion risk.

Promising extensions include incorporating exogenous covariates (weather, tidal state, scheduled arrivals) to improve recall, multi-step-ahead prediction via recursive temporal unrolling, and complementing z -score evidence with gradient-based SHAP [7] or GNNExplainer [5] attributions for multi-method corroboration. Deployment in a real-time operational dashboard remains the ultimate validation target.

REFERENCES

- [1] Port of Los Angeles, “Port of Los Angeles container statistics,” Port of Los Angeles, Los Angeles, CA, USA, 2023. [Online]. Available: <https://portoflosangeles.org/business/statistics/container-statistics>
- [2] A. Komaromi, D. A. Cerdeiro, and Y. Liu, “Supply chains and port congestion around the world,” Int. Monetary Fund, Washington, DC, USA, Working Paper WP/22/59, Mar. 2022, doi: 10.5089/9798400206481.001.
- [3] M. Liang, R. W. Liu, Y. Zhan, H. Li, F. Zhu, and F.-Y. Wang, “Fine-grained vessel traffic flow prediction with a spatio-temporal multigraph convolutional network,” *IEEE Trans. Intell. Transp. Syst.*, vol. 23, no. 12, pp. 23694–23707, Dec. 2022, doi: 10.1109/TITS.2022.3200730.
- [4] Peng, W., Bai, X., Yang, D., Yuen, K. F., & Wu, J. (2023). A deep learning approach for port congestion estimation and prediction. *Maritime Policy & Management*, 50(7), 835–860. <https://doi.org/10.1080/03088839.2022.2057608>
- [5] R. Ying, D. Bourgeois, J. You, M. Zitnik, and J. Leskovec, “GNNExplainer: Generating explanations for graph neural networks,” in *Adv. Neural Inf. Process. Syst. (NeurIPS)*, vol. 32, Vancouver, Canada, 2019, pp. 9240–9251.
- [6] P. Veličković, G. Cucurull, A. Casanova, A. Romero, P. Liò, and Y. Bengio, “Graph attention networks,” in *Proc. 6th Int. Conf. Learn. Represent. (ICLR)*, Vancouver, Canada, 2018. [Online]. Available: <https://openreview.net/forum?id=rJXMpikCZ>
- [7] S. M. Lundberg and S.-I. Lee, “A unified approach to interpreting model predictions,” in *Adv. Neural Inf. Process. Syst. (NeurIPS)*, vol. 30, Long Beach, CA, USA, 2017, pp. 4765–4774.
- [8] D. Chen, C. Huang, T. Fan, H. C. Lau, and X. Yan, “Predictive modelling for vessel traffic flow: A comprehensive survey,” *Transp. Saf. Environ.*, 2025, doi: 10.1093/tse/tdaf022.